

Observation of machined surface and subsurface structure of hinoki (*Chamaecyparis obtusa*) produced in slow-speed orthogonal cutting using X-ray computed tomography

Yosuke Matsuda · Yuko Fujiwara ·
Yoshihisa Fujii

Received: 21 September 2014 / Accepted: 12 December 2014 / Published online: 1 January 2015
© The Japan Wood Research Society 2014

Abstract X-ray computed tomography (CT) was applied to non-destructive observation of machined surface and subsurface structure of hinoki (*Chamaecyparis obtusa*) produced in slow-speed orthogonal cutting. The cutting experiments were conducted under several cutting conditions and the chip formations were observed with a high-speed camera to be classified into four chip types. The difference in the quality of the machined surfaces produced in four types of chip formation was investigated. During type 0 chip formation, the workpiece was cut almost exactly at the path of the cutting edge, so no deformation was found on and beneath the machined surface. During type I chip formation, the direction of the fore-split, which is dependent on the arrangement of cells, determined the machined surface. During type II chip formation, the cutting tool sometimes tore part of the workpiece below the path of the cutting edge and the tore part was then compressed by the tool, remaining on the machined surface. During type III chip formation, part of the workpiece above the path of the cutting edge was compressed by the tool, instead of being removed as a chip, so the compression occurred in wide area. The relationship between the formation of the machining defects such as torn grain or the compressed cells and the way chip is separated, deformed, or removed was clarified in this study.

Keywords Chip type · Orthogonal cutting · Surface quality · X-ray computed tomography

Introduction

In a wood cutting process, a series of small destructions occur in the wood ahead of a sharp edge of a cutting tool as the cutting edge passes. The wood above the path of the edge is removed as a chip, and a new machined surface is produced.

One of the purposes of wood cutting is to obtain satisfactory machined surface. The machined surface of good quality is considered to be formed when the workpiece is cut exactly at the path of the cutting edge, meaning that the workpiece above the path of the edge is completely removed and no machining defects such as torn grain, fuzzy grain, or any other destructions would be found. In addition, as Scholz et al. [1] mentioned, no compressed cells should be found on and beneath the surface, since they may absorb moisture and swell, causing rough surface. Some studies have been done observing both the machined surface and subsurface structure; although the workpiece was cut at a plane normal to the machined surface to be observed with microscope, so the procedure was destructive and might have changed shapes of cells observed [2–4].

On the other hand, many studies of wood cutting have been conducted, aiming to optimize the formation of the satisfactory machined surface under different cutting conditions. In those studies, stresses and strains of wood and resultant cutting forces have been measured and analyzed [5–11]. Most importantly, Franz [12, 13] and McKenzie [14] have classified chip formation in orthogonal cutting process parallel to the grain into chip types, based on the way chips being separated, deformed, and removed, and

A part of this article was presented at the 64th Annual Meeting of the Japan Wood Research Society, Matsuyama, Japan, March 2014.

Y. Matsuda (✉) · Y. Fujiwara · Y. Fujii
Graduate School of Agriculture, Kyoto University,
S-220 Nougakubu-Sougohkan, Kitashirawaka-oiwake-cho,
Sakyo-ku, Kyoto, Kyoto 606-8502, Japan
e-mail: yosuke@h3news1.kais.kyoto-u.ac.jp

the relation of the types to the cutting condition such as depth of cut and cutting angle has been investigated. Their studies are remarkable since those were the first studies to categorize chip formation during the cutting and their definition for each type has been used since then.

Some studies have investigated relationship of chip types to the resultant cutting force [15, 16], although the relation between the types and surface quality is not deeply discussed in these studies. Franz [12, 13] mentioned that the machined surface produced in type II chip formation is so-called of good quality. However, Franz has not conducted type 0 chip formation and it is unknown whether type II is superior or not to type 0 in terms of the surface quality. McKenzie et al. [17] conducted both inclined and orthogonal cutting, and found that changes in the occurrence of chip type induced by the inclination affect the surface quality. However, only the occurrence of defects such as raised grain or torn grain on the surface has been checked in their study, so it is uncertain whether the compressed cells, which Scholz et al. [1] mentioned, appear or not on and beneath the machined surface of each chip type.

In this study, orthogonal (90–0) cutting was conducted under several cutting conditions, and both the machined surface and subsurface structure were observed non-destructively with micro focus X-ray computed tomography (CT) system. The relation of the quality of machined surface and subsurface structure to cutting angle and depth of cut, especially difference in the appearance of the compressed cells among the chip type, was investigated.

Materials and methods

Forty pieces of air-dried hinoki (*Chamaecyparis obtusa*), of 5 mm wide in radial (R) direction, 50 mm long in longitudinal (L) direction, and 50 mm high in tangential (T) direction, were used as workpieces. The average air-dry density was 0.38 g/cm³ and the average moisture content was 10.6 %. Four cutting tools with wedge angles of 25°, 45°, 65°, and 85° were employed. The tools were made of high-speed steel (SKH51), and their rake faces were coated with chromium nitride. The coating was about 5 μm thick.

Orthogonal cutting experiment was conducted on a milling machine equipped with a motorized linear feed stage on the machine's table (Fig. 1). The workpiece was mounted on the feed stage, and was fed at a constant speed of 5 mm/s toward the cutting tool which was fixed to the overarm of the milling machine. The machined surface was RL surface normal to tangential direction, that is, quarter-sawn surface. The cutting tool was fed in the longitudinal direction (90–0 cutting) without bias angle.

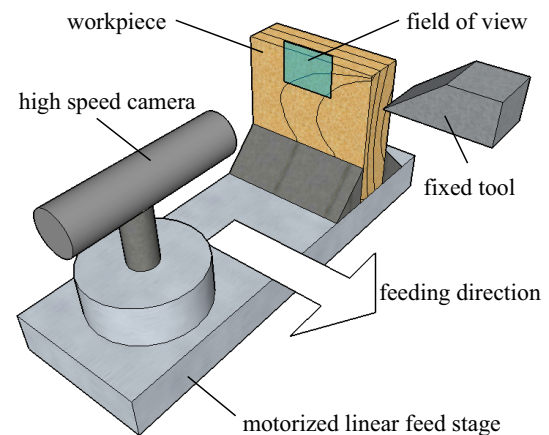


Fig. 1 Schematic illustration on experimental apparatus

Depth of cut and cutting angle were varied so as to generate chips of types 0 to III. The depths of cut employed were 0.1 and 0.3 mm. The clearance angle was kept constant at 5°, so the cutting angles employed were 30°, 50°, 70°, and 90°. The total combination of the depth of cut and the cutting angle was eight. The cutting was conducted five times for each cutting condition, so the cutting experiments were conducted forty times in total, and the workpiece was exchanged randomly for each cutting.

The process of chip formation during the cutting was taken as a video clip with a high-speed camera (VW-6000, KEYENCE). The video clips were recorded at a shutter speed of 1/1000 s and a frame rate of 250 fps. The lens unit of the camera was fixed on the feed stage perpendicularly to the feeding direction and moved together with the workpiece, so that the camera would always take pictures of a certain area of the side surface of the workpiece. The field of view of the camera was approximately 3.8 mm in width and 2.6 mm in height. The video clip was analyzed to determine the chip type occurred during the cutting.

After the cutting experiments, the machined surface and subsurface structure of all workpieces were scanned by a micro focus X-ray CT system (SMX-160CT-SV3S, SHIMADZU). Two scanning conditions (a) and (b) were applied for the scanning. For scanning condition (a), the size of the field of view was 6.2 mm in both R and T directions, and 5.8 mm in L direction, and the voxel size of the tomogram was 12 μm. The width of the field of view in R direction was wider than the thickness of the workpiece, although the detailed appearance of cells could not be observed. On the other hand, for scanning condition (b), field of view was 1.4 mm in all three directions, and the voxel size was 2.7 μm. The lumens of the cells could be observed in this condition, although the field of view was limited. For both scanning conditions, the length of the field of view in L direction was not long enough to scan the

entire machined surface, so that a part of the whole machined surface was scanned and investigated.

Results and discussion

All chip formations found in this study were categorized into four chip types defined by Franz [12, 13] and McKenzie [14]. Figure 2 shows pictures of chip formation of each chip type taken by the high-speed camera. (a), (b), (c), and (d) in Fig. 2 represent type 0, I, II, and III, respectively. The cutting angles for (a) to (d) were 30°, 50°, 70°, 90°, respectively. The depth of cut was 0.1 mm for (a), while 0.3 mm for (b), (c), and (d). Table 1 shows the occurrence of the chip type for various combinations of cutting angle and depth of cut. The relationship between the chip type and the cutting condition was similar to those of previous studies [13, 16]. It was confirmed that only one chip type occurred for each cutting condition in the most of the cases. When the cutting angle was 50° and the depth of cut was 0.1 mm, however, chip type varied itself among the types 0, I, and II in the five repetitions. This cutting

Table 1 Occurrence of chip types under various combinations of cutting angle and depth of cut

Depth of cut (mm)	Cutting angle (°)			
	30	50	70	90
0.1	0	0, I, II	II	III
0.3	I	I	II	III

condition was at a boundary among the chip type occurrence.

Type 0 chip was obtained when cutting angle was 30° and depth of cut was 0.1 mm, and also when the boundary condition was employed. In the video clip, the chip split at the distance of 0.01 mm or closer from the cutting edge, and no deformation could be observed on the workpiece beneath the path of the cutting edge (Fig. 2a).

Figure 3 shows the CT images of one of the machined workpieces produced in type 0 chip formation. The cutting angle employed was 30° and the depth of cut employed was 0.1 mm for this workpiece. The intensity of a pixel in a CT image represents the density level of the pixel; the

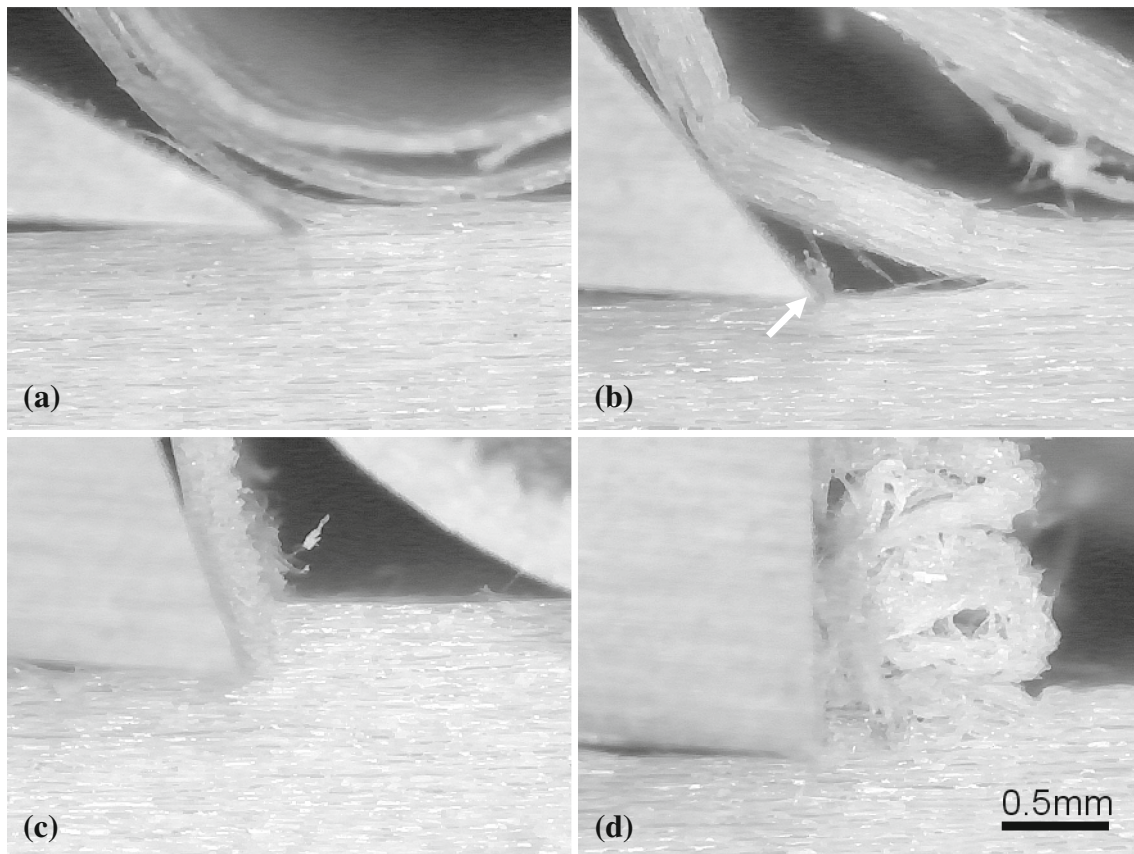


Fig. 2 Chip formations of each chip types. **a** Type 0. **b** Type I. **c** Type II. **d** Type III. The *white arrow* indicates the secondary chip. Cutting angles for (a) to (d) were 30°, 50°, 70°, 90°, respectively. Depth of cut was 0.1 mm for (a), while 0.3 mm for (b), (c), and (d)

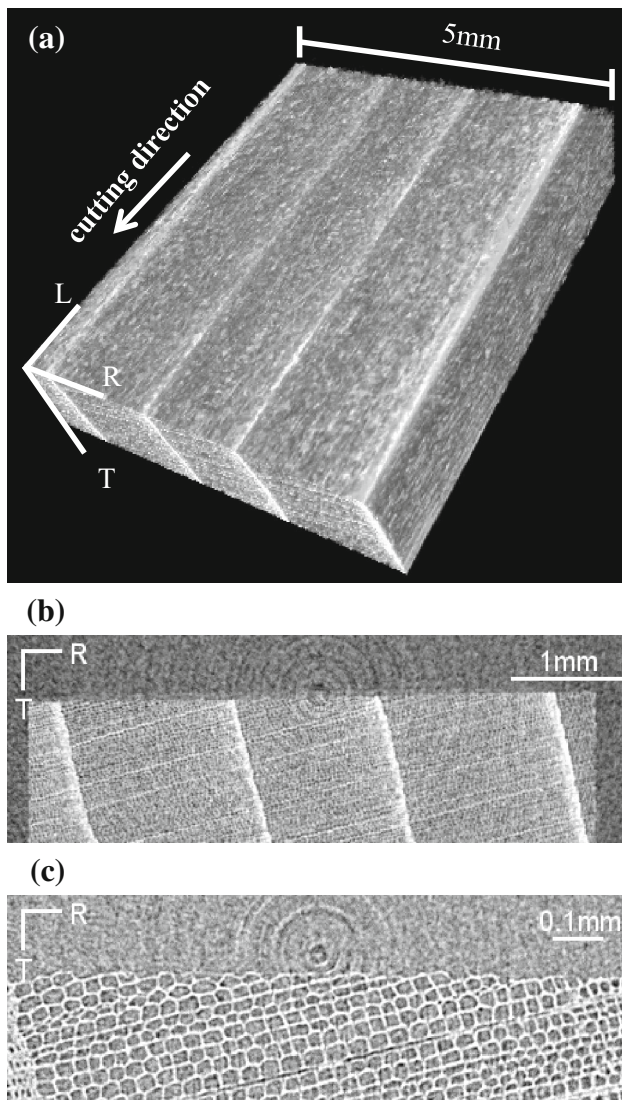


Fig. 3 CT images of the machined workpiece obtained by type 0 chip formation. Cutting angle was 30° and depth of cut was 0.1 mm. **a** 3D view of the workpiece. **b**, **c** cross-sectional view (RT plane) of the workpiece

brighter the pixel is, the higher the density of the pixel is. Figure 3a shows a 3D rectangular prism image of a part of the workpiece. RL plane indicates the machined surface, while LT plane indicates the side surface of the workpiece. RT plane indicates a cross-sectional view, which is vertical to the cutting direction, of the workpiece. Figure 3b, c shows the cross-sectional views of the rectangular prism. Figure 3b was scanned by scanning condition (a), while Fig. 3c was scanned by scanning condition (b). The surfaces parallel to R direction in Fig. 3b, c are the machined surface. The two bright stripe-like zones running vertically from the machined surface in Fig. 3b are the latewood of the annual rings. The cells on the machined surface were cut almost exactly at the path of the cutting edge, as shown

in Fig. 3b. Most of the cells on and beneath the machined surface seemed to be neither compressed nor deformed, as shown in Fig. 3c. In addition, it was confirmed that the cut was mostly done along the intercellular layer. The characteristics of the surface and subsurface structure of type 0 observed with X-ray CT correspond to the fact that no deformation of the workpiece was observed in the video clip of type 0.

Type I chip was obtained when the cutting angle was 30° or 50° and the depth of cut was 0.3 mm, and also when the boundary condition was employed. The chip split along the grain by cleavage and failed as if a cantilever beam bends and breaks down at its base, as shown in Fig. 2b. Splitting of workpiece near the cutting edge was in a larger scale than that of type 0, occurred at the distance of 0.1 mm or further from the cutting edge. This splitting is designated as “fore-split”. The generated chip slid up the rake face of the tool until the cutting edge reached the next contact point of the workpiece. This phenomenon repeated in the cutting process. In some cases, the split proceeded above the path of the cutting edge, and the uncut part above the path of the edge was removed as a secondary chip, as pointed by the white arrow in Fig. 2b. The secondary chip was thin and similar to the type II chip, as Franz mentioned [12].

Figures 4 and 5 show the CT images of the machined workpieces produced in type I chip formation. The cutting angle was 50° and the depth of cut was 0.3 mm for the workpiece in Fig. 4, while the cutting angle was 30° and the depth of cut was 0.3 mm for the workpiece in Fig. 5. A couple of bright spots of higher density were found on the surface, as pointed by the white arrows in Fig. 4b, c. These bright spots must be the masses of the compressed cells. The cells were seriously deformed, and no cell lumens could be observed (Fig. 4c). These compressed areas were considered to be produced by the secondary chip formation of type II, since similar areas were also found on the machined surfaces of type II. For the workpieces whose contact angle of annual ring was smaller than the right angle, the fore-split tended to lead below the path of the cutting edge. Therefore, the machined surface seemed not to match the path of the cutting edge, as pointed by a white triangle in Fig. 4c. On the other hand, when the contact angle of annual ring was close to 90° , the machined surfaces were similar to those of type 0, and seemed to match the path of the cutting edge (Fig. 5b, c). In both cases, the chip tended to split along the intercellular layer. It was confirmed that the direction of the fore-split, which was dependent on the arrangement of cells, determined the machined surface.

Type II chip was obtained when the cutting angle was 70° , and also when the boundary condition was employed. During the chip formation, the workpiece above the path of

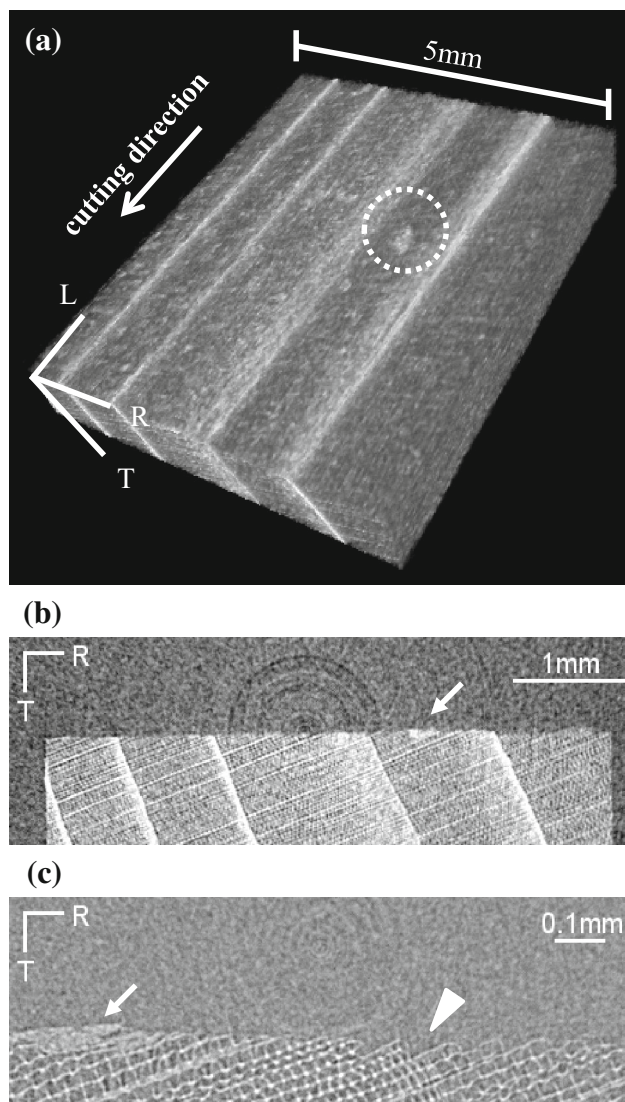


Fig. 4 CT images of the machined workpiece obtained by type I chip formation. Cutting angle was 50° and depth of cut was 0.3 mm. The circled area in **a** and the bright areas pointed by white arrows in **b** and **c** indicate the compressed areas. White triangle in **c** indicates a poor surface

cutting edge failed along a line extending upward from the edge, while the workpiece below seemed to be not deformed. This phenomenon probably induced by a shearing stress along the inclined line. In the video clip, no fore-split could be observed (Fig. 2c), and the cutting edge seemed to control the chip formation.

Figure 6 shows the CT images of one of the machined workpieces produced in type II chip formation. The cutting angle was 70° and the depth of cut was 0.1 mm. Most of the areas of the machined surface appeared to match the path of the cutting edge (Fig. 6c), as seen from the video clip. No torn grain or fuzzy grain was found (Fig. 6a). As

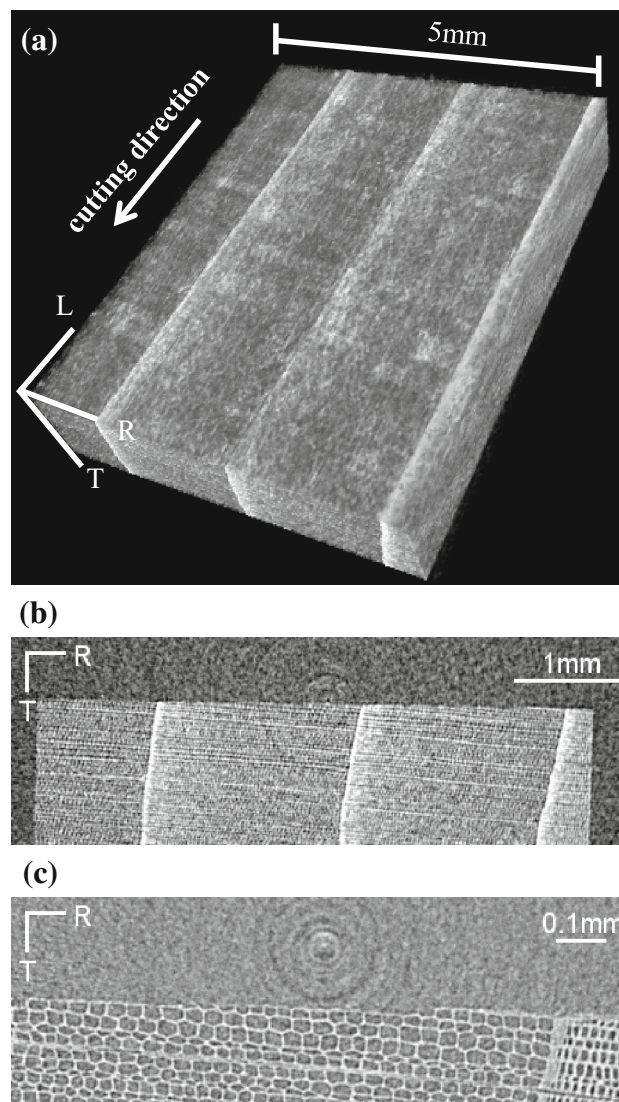


Fig. 5 CT images of the machined workpiece obtained by type I chip formation. Cutting angle was 30° and depth of cut was 0.3 mm

pointed by the white arrow in Fig. 6b, however, the bright spots were found.

Figure 7 shows the CT images of another workpiece of type II. The cutting angle was 70° and the depth of cut was 0.3 mm. Figure 7b is a cross-sectional view (LT plane) of the workpiece, which was scanned by scanning condition (b). The cutting edge first passed across the dotted line (c), then across the dotted line (d), where the workpiece seemed to be torn, and finally the dotted line (e), where the compressed area was observed. This indicates that after the workpiece below the path of the cutting edge was torn, it was compressed and remained on the surface, instead of being removed as a chip. This compressed area accompanied with the tore area seems to be a characteristic of type II chip formation, although it should be investigated more in detail.

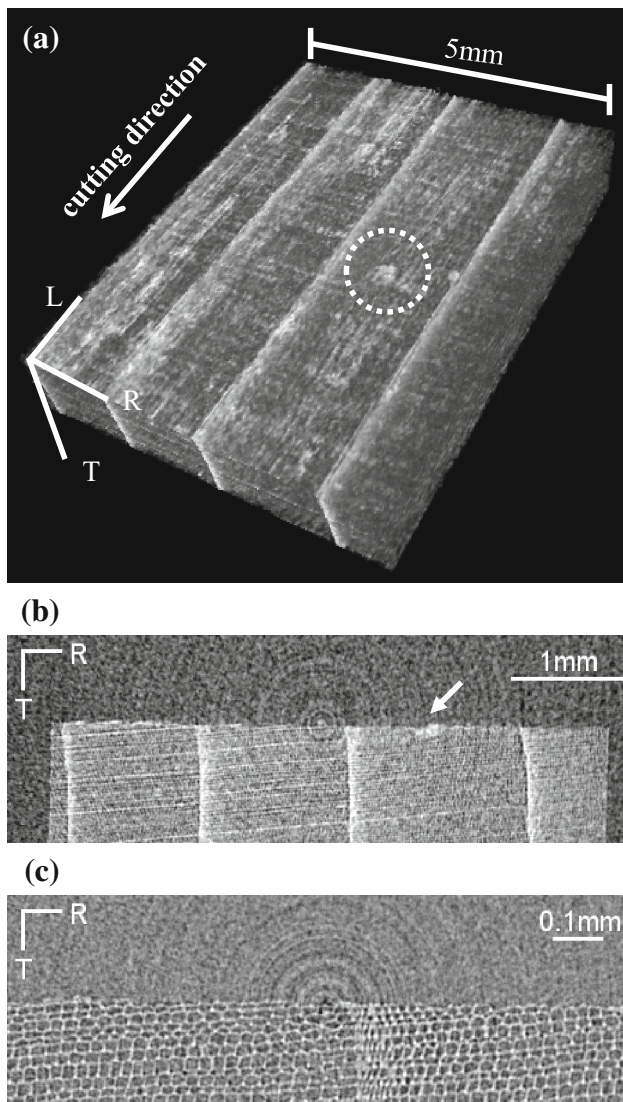


Fig. 6 CT images of the machined workpiece obtained by type II chip formation. Cutting angle was 70° and depth of cut was 0.1 mm. The circled area in **a** and the bright area pointed by white arrow in **b** indicate the identical compressed area

Type III chip was obtained when the cutting angle was 90° . The workpiece ahead of the tool was compressed by the tool and the compressed zone usually extended below the machined surface. The chip generated was also compressed and seriously damaged, and frequently stuck to the rake surface (Fig. 2d). Since the chip tended to stick ahead of the tool, the cutting was not only done by the cutting edge but also by the stuck chip, which made the cutting unstable. When the chip made the cutting angle larger than 90° , the workpiece above the path of the cutting edge seemed to be compressed and passed beneath the clearance face instead of removed along the rake surface. Those parts of the workpiece would be compressed and would be left on the machined surface.

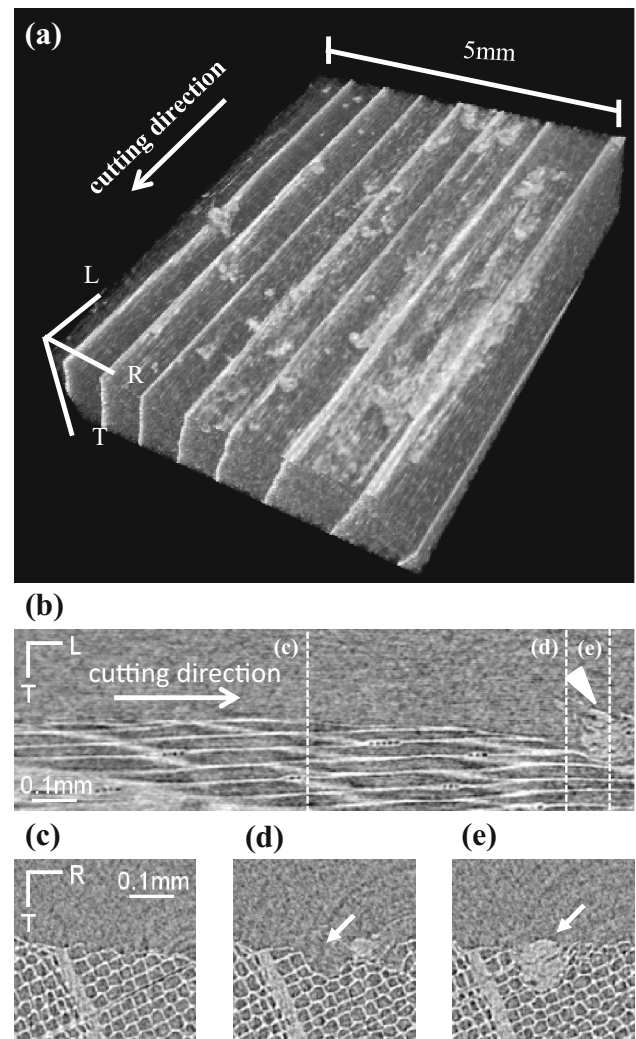


Fig. 7 CT images of the machined workpiece obtained by type II chip formation. Cutting angle was 70° and depth of cut was 0.3 mm. **b** a cross-sectional view (LT plane) of the workpiece. **c**, **d**, and **e** are cross-sectional views (RT plane) sliced at the dotted lines (**c**), (**d**), and (**e**) in **b**, respectively. White triangle in **b** and white arrow in **e** indicate the identical compressed area. White arrow in **d** indicates the accompanied tore area

Figure 8 shows the CT image of one of the machined workpieces produced in type III chip formation. The cutting angle was 90° and the depth of cut was 0.3 mm. Occurrence of fuzzy grains was found in the most of workpieces, as pointed by the white arrows in Fig. 8a. The surface seemed not to match the path of the cutting edge. Wide area of the surface was covered with the compressed cells in the most of workpieces, as shown in Fig. 8b, c. The appearance of the compressed surface was typical to type III chip formation, as McKenzie [14] mentioned.

It was revealed in this study that type 0 chip formation was better than any other types in terms of surface quality. The chip formation was done at the point very close to the

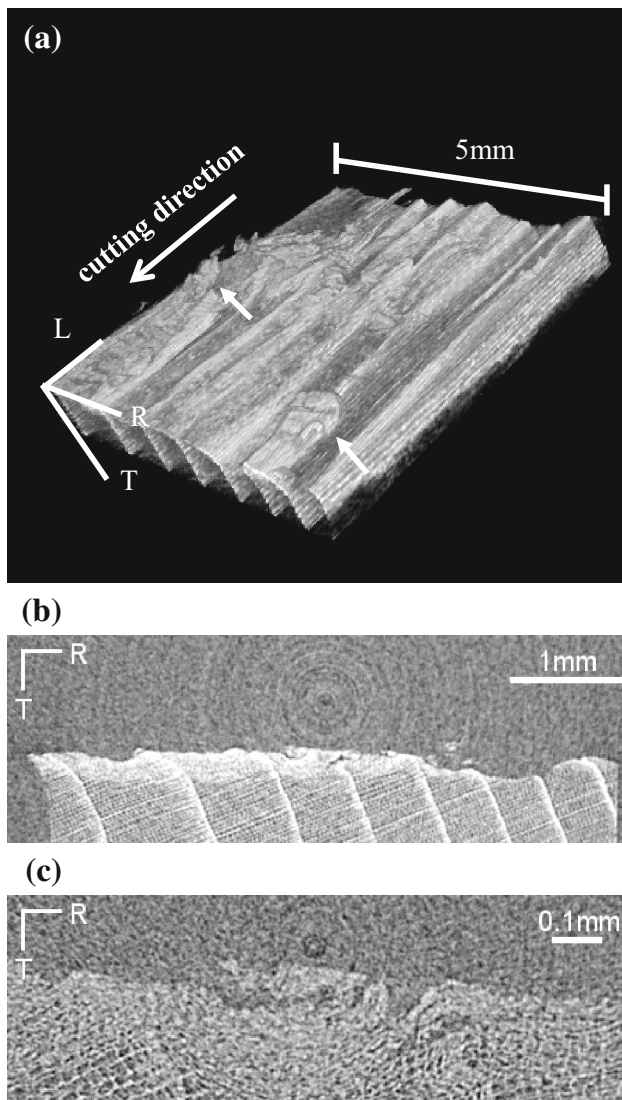


Fig. 8 CT images of the machined workpiece obtained by type III chip formation. Cutting angle was 90° and depth of cut was 0.3 mm. White arrows indicate fuzzy grains

cutting edge without any deformation in the workpiece below the cutting edge, and the workpiece above the path of the cutting edge was completely removed. However, the cutting tool for type 0 chip formation is improper for the practical wood machineries. The cutting angle for type 0 must be very small, so the tool may not withstand the intermittent and high impact caused in a high-speed cutting and will soon become blunt. It may be better for the practical use to employ cutting condition for type II, since the cutting angle is relatively high and the machined surface seems to match the path of the cutting edge, although finding out the way to prevent the occurrence of the compressed areas is necessary for employing type II chip formation.

Conclusion

The slow-speed orthogonal cuttings under several cutting conditions were observed with a high-speed camera, and both the machined surface and subsurface structure were observed non-destructively with a micro focus X-ray CT system. The relation of the quality of the machined surface and of the subsurface structure to the chip types was investigated.

The machined surface appeared to match the path of the cutting edge when the cutting condition for type 0 or II chip formation was employed. On the other hand, the surface of type I seemed not to match the path of the cutting edge, depending on the contact angle of annual ring to the workpiece surface. The compressed cells were found on and beneath the machined surfaces of type I and II. Those compressed cells seemed to be generated, as a part of the workpiece that was torn, compressed by the cutting edge, and finally remained on the surface. These compressed areas were not found on and beneath the machined surface of type 0. These results led us to conclude that type 0 is the most satisfactory in terms of surface quality. However, the cutting condition for type 0, employing thin cutting edges, is not always practical for the ordinal high-speed wood machining.

Using the X-ray CT system, it was possible to observe the quality of machined surface and the subsurface failures non-destructively. The method used in this study may become a new method for evaluating the wood machinability.

Acknowledgments Authors would like to express sincere thanks to Kanefusa Corporation for providing the cutting tools.

References

- Scholz F, Laugel J (2001) Compression of the surface layer by up milling and detection methods. In: Proceedings of the 15th International Wood Machining Seminar, 30 Jul- 1 Aug, 2001, Los Angeles, pp 419–436
- Hayashi D, Tochigi T, Yamazaki M (1970) Studies on veneer cutting at the cellular level: rupture formation of cell walls. *Mokuzai Gakkaishi* 16:70–75
- Stewart HA, Crist JB (1982) SEM examination of subsurface damage of wood after abrasive and knife planing. *Wood Sci* 14:106–109
- Kuljich S, Cool J, Hernández RE (2013) Evaluation of two surfacing methods on black spruce wood in relation to gluing performance. *J Wood Sci* 59:185–194
- Hoadley RB (1968) Strain analysis in wood by means of moiré patterns. *Forest Prod J* 18:48–50
- McKenzie WM (1969) Applying grid patterns to wood surface using photosensitive lacquers. *Forest Prod J* 19:43–44
- McKenzie WM, Karpovich H (1975) Measured strains in slow linear veneer cutting: effects of nosebar form and gap. *Wood Sci and Technol* 9:213–231

8. Sugiyama S (1975) Fundamental studies on mechanism of veneer cutting VII: numerical analysis of stress distribution in workpiece during cutting without pressure bar. *Mokuzai Gakkaishi* 21:15–21
9. Palka LC (1975) Veneer-cutting analysis by an elastic finite-element model: a case study. *Wood Sci* 8:97–104
10. Kinoshita N (1983) Analysis of the veneer-formation process II: numerical analysis of cutting stress in lathe check formation by finite element method. *Mokuzai Gakkaishi* 29:877–883
11. Kinoshita N (1984) Analysis of the veneer-formation process III: analysis of cutting stress by the photo elastic coating method. *Mokuzai Gakkaishi* 30:32–37
12. Franz NC (1955) Analysis of chip formation in wood machining. *Forest Prod J* 5:332–336
13. Franz NC (1958) Analysis of the wood-cutting process. Dissertation, University of Michigan, USA
14. McKenzie WM (1967) The basic wood cutting process. In: *Proceedings of the Second Wood Machining Seminar*, Oct 10–11 1967, Richmond, pp 3–8
15. Stewart HA (1971) Chip formation when orthogonally cutting wood against the grain. *Wood Sci* 3:193–203
16. Inoue H, Mori M (1979) Effects of cutting speed on chip formation and cutting resistance in cutting of wood parallel to the grain. *Mokuzai Gakkaishi* 25:22–29
17. McKenzie WM, Hawkins BT (1966) Quality of near longitudinal wood surfaces formed by inclined cutting. *Forest Prod J* 16:35–38